








METHODOLOGY

Open Access



# Protocol for the production of micro- and nanoplastic test materials

Luke A. Parker<sup>1\*</sup> , Elena M. Höppener<sup>1</sup> , Edward F. van Amelrooij<sup>1</sup>, Sieger Henke<sup>1</sup> , Ingeborg M. Kooter<sup>1</sup> , Kalouda Grigoriadi<sup>2</sup> , Merel G. A. Noojens<sup>2</sup>, Andrea M. Brunner<sup>1</sup>  and Arjen Boersma<sup>2</sup> 

## Abstract

Micro- and nanoplastics (MNP) are ubiquitous, but little is known about the risks they pose to human health. Currently available data are of limited use for developing relevant risk assessments due to poor quality control, the lack of a standardised approach to particle characterisation and environmental analysis, and the use of test materials that do not reflect those found in the environment. A set of well-characterised MNP test materials would greatly alleviate this. Here, we present a robust method to produce, fractionate and characterise such test materials of PP and PVC. Initial size reduction of commercial powders or pellets to 500 µm was performed using a centrifugal mill under cryogenic conditions. Further ball-milling between room temperature and -50 °C in 1-propanol was then performed to reach the final particle sizes. Fractionation into size ranges of < 1, 1–5, 5–10, 10–30, 90–180 and 180–300 µm was performed by sedimentation and filtration. Characterisation of the reference materials through SLS, SEM–EDX, XRF and TGA demonstrated that the fractions were of the desired size and levels of contamination from the procedure were < 1 wt%. Stability testing in both 1-propanol and 0.05 wt% BSA solution showed that whilst some agglomeration occurred during storage in 1-propanol the suspensions were stable in BSA over 9 months and some of the previous agglomeration was reversed.

**Keywords** Microplastics, Nanoplastics, Reference material, Environmental analysis, Nanoparticles, Test particles

## Introduction

Micro- and nanoplastics (MNPs), plastic particles < 5 mm and < 0.1 µm, respectively [1, 2], are seen as a potential health risk due to their abundance and persistence in the environment [3, 4]. Since the beginning of this millennium, > 6000 research papers have been published on the environmental presence of MNPs (Scopus: microplastic OR nanoplastic; since 2000; Subject area “Environmental Science; Document type “Article”). They have been shown to be present in not only various environmental compartments (seas, lakes and rivers, air, soil,

and glaciers) [5–8], but also in plants and animals [9, 10]. More recently, MNPs have also been detected in the human body, including in the blood [11] and the placenta [12]. Whilst their presence in the human body has been demonstrated, the health effects related to this remain poorly understood and are therefore the topic of many studies [13–17].

A number of recent literature reviews have concluded that current data are insufficient to draw conclusions on the health effects of microplastics in humans and animals [18–20]. Common reasons for this are the use of insufficiently characterised particles (relying on manufacturer information without independent analysis of size, shape and polymer type) and/or particles that do not reflect those found in the environment [21]. The particles used may differ to environmental particles in their shape, plastic type, size, or presence of (surface) modifiers such as surfactants. For instance, two thirds of all studies

\*Correspondence:

Luke A. Parker

luke.parker@tno.nl

<sup>1</sup> TNO Environmental Modelling, Sensing and Analysis, Princetonlaan 6-8, 3584 CB Utrecht, Netherlands

<sup>2</sup> TNO Material Solutions, HTC 25, 5656 AE Eindhoven, Netherlands

investigating the effects on aquatic biota used spherical MNPs, despite the fact that these account for only ~6% of environmental MNP [22]. The polymer types most often used in the literature are polystyrene (PS) or polyethylene (PE) resulting in their overrepresentation compared to other plastics. In contrast, polypropylene (PP) has been found in more than 50% of studies looking at fresh and drinking waters [5], but is only investigated in 6% of effect studies [18]. Furthermore, as some particles used in health studies have surfactants present at their surface, the effects observed might be a result of the surfactants causing for example cell lysis [23]. Thus, in order to study the health effects of polymer type and particle sizes, it would be beneficial to study particles with a well-defined size fractionation and without any modified surfaces (e.g. without surfactants).

Nanoplastics present a unique problem as a lack of analysis capabilities mean there is also little known about their abundance and the properties they may have [24]. Whilst nanobeads of <1 µm are frequently used for effect testing, their presence in the environment is still unknown. Environmental MNPs are a broad size distribution spanning seven orders of magnitude from nanometres to millimetres, however this broad distribution is not reflected in the current test materials with only 16% of studies investigating a size range greater than one order of magnitude [18].

To allow for the development of proper MNP risk assessments, it is instrumental that the MNP test materials used in exposure studies accurately represent those found in the environment [25]. We consider environmentally relevant test materials to be satisfying the following three conditions: i) fragment or fibre particle morphology; ii) good size fractionation across a wide size range; and iii) no modification of the plastic surface. There have been numerous studies that report the production of reference plastic particles. In these studies there are mainly two production methods described, either employing a bottom-up approach using dissolution and precipitation processes [26–29] or a top-down approach using mechanical degradation steps (e.g. milling) [30–32]. Whilst these studies provide very useful testing materials for different scenarios, none of them satisfy all three conditions for being considered environmentally relevant. Some studies are limited in terms of particle size fractionation and report a limited size distribution. For example, the milling method developed by Seghers et al. produces a reference material between 30–200 µm but does not show the possibility to produce nanoplastics [32], whereas the bottom up approaches by Rodríguez-Hernández[27] and Balakrishnan[28] produce nanoplastic reference materials but not microplastics. Furthermore, particles generated from bottom-up

approaches are sometimes spherical as opposed to fragments [26]. These particles are of great value for investigating the effects of nanoplastics or microplastics but do not allow for correlation across orders of magnitude. Likewise, other studies modify the plastics by using metal-dopants[29] or fluorescent labels[31] and whilst this is very beneficial for tracking and recovery purposes, it leads to the possibility of modified material properties. Finally, surfactants are often used to stabilise reference materials against agglomeration, however these modify the particle surface [28, 32].

In this work we detail the development of a method for the production of relevant MNPs test materials in distinct size fractions of <1, 1–5, 5–10, 10–30, 90–180 and 180–300 µm. Production was performed through a two-step milling process involving an initial coarse size reduction step using a rotary mill followed by intensive ball-milling with duration and temperature dependent on plastic properties. The prepared materials were then fractionated through sedimentation and wet sieving, and concentrated to produce a standard dispersion of 20 mg/ml MNP/1-propanol. The resulting materials were thoroughly characterized by static light scattering (SLS), scanning electron microscopy with energy dispersive x-ray spectroscopy (SEM–EDX), thermogravimetric analysis (TGA) and x-ray fluorescence (XRF) to determine size, morphology, chemical composition and dispersion stability in both storage and in the presence of bovine serum albumin (BSA) (a main constituent of common cell culture medium). We have demonstrated the method for PVC and PP/Talc, however we envisage that this can be easily adapted to produce test materials of many plastic materials.

The procedure from starting material to concentrated MNP fractions takes approximately 50–80 h (max. 24 h milling, 24–48 sedimentation, 1–2 h sieving, 1–2 h centrifugation) and is accomplishable with no specialised equipment. We expect (although have not tested) that the rotary mill can be replaced by other coarse milling techniques, as long as the particle size is sufficiently reduced, however, long duration ball-milling is crucial to produce the smallest size fractions. Ball-milling parameters will need to be optimised for each lab depending on equipment and also per plastic type and possibly per plastic grade due to the varying material properties. Likewise, sieving needs to be optimised per lab to achieve the best possible fractionation of particles with attention to the use of sonication and over/under pressure to achieve this.

## Results and discussion

### Milling and fractionation of MNP test materials

The starting materials for the process, PP/Talc and PVC, were commercial polymers in pellet and powder form,

respectively. As most MNP exposure tests are performed in aqueous solutions, the particles must sediment on the target cells. As all polyolefins (e.g. PE and PP) have a density lower than 1 g/ml, the density of the PP needed to be increased. This was achieved by adding 30 wt% nano-talc as a filler during the extrusion step. Talc was chosen as it is frequently used as a mineral filler in commercial PP to modify material properties [33]. As the talc content in commercial PP can be as high as 40 wt%, we were able to use a PP/Talc that sinks whilst remaining environmentally relevant [34]. The final density of the 30 wt% PP/Talc was 1.13 g/cm<sup>3</sup>.

In order to produce MNP test materials in the desired fractions of <1, 1–5, 5–10, 10–30, 90–180 and 180–300 μm, a four-step process was devised. This is illustrated in Fig. 1. First, the PP/Talc pellets were reduced in size to below 500 μm in a centrifugal mill (1). Then the powder was further ground in a ball mill (2). The resulting dispersions were then fractionated using sedimentation (3) followed by sieving (4). The final fractions were concentrated to the required 20 mg/ml using ultracentrifugation.

The first grinding step in the centrifugal mill is intended for a coarse particle reduction that should increase the efficiency of the subsequent ball-milling. In the grinding step, a stainless steel mesh screen encircles the rotating blades allowing particles under a certain size to pass through while larger particles remain inside for further size reduction. For PVC this step was carried out at room temperature, whilst for the more ductile PP/Talc it was carried out under liquid N<sub>2</sub> (LN<sub>2</sub>) to embrittle the polymer and enhance grinding efficiency. For both polymers, a 500 μm screen size was used.

The subsequent ball-milling step reduces the MNP further to the final size. In this step, Y-stabilised ZrO<sub>2</sub> balls are used in a ZrO<sub>2</sub> vessel with a ZrO<sub>2</sub> stirrer. For PVC, milling can proceed for 20–25 h at room temperature, however for the more ductile PP/Talc, LN<sub>2</sub> is again required to reach the required size. The LN<sub>2</sub> must be topped up every 10–20 s and milling time is limited to 1 h. A summary of the batches milled and the milling conditions used is presented in Table 1.

After grinding, all dispersions were converted to 1-propanol by replacing the ethanol in those experiments where it was used during the grinding step. This was done by diluting the dispersion with 1-propanol, centrifuging and decanting the supernatant four times. No major differences in particle size were observed between the batches milled in ethanol and 1-propanol. The dispersions for each polymer were then combined and diluted

**Table 1** Summary of the PVC and PP/Talc batches that have been milled in the Dispermat Ball Mill

Batch	Mass	Mass ZrO <sub>2</sub> beads (1 mm)	Milling time	Conditions
PVC_BI	72 g	1100 g	20 h @ 6000 rpm	RT, ethanol
PVC_BII	72 g	1100 g	20 h @ 6000 rpm	RT, ethanol
PVC_BIII	90 g	1200 g	20 h @ 6000 rpm	RT, ethanol
PVC_BVI	60 g	1000 g	25 h @ 3000 rpm	RT, 1-propanol
PP/Talc_BV	50 g	1130 g	65 min @ 2000 rpm	LN <sub>2</sub> , 1-propanol
PP/Talc_BVII	32 g	600 g	60 min @ 2000 rpm	LN <sub>2</sub> , 1-propanol
PP/Talc_BVIII	30 g	600 g	60 min @ 3000 rpm	LN <sub>2</sub> , 1-propanol

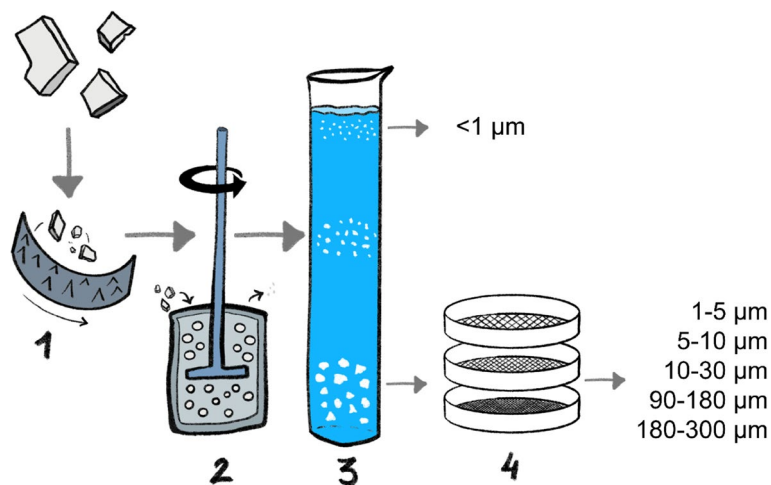


**Fig. 1** Procedural scheme for Milling and Fractionation of MNP Test Material. Steps: 1. Centrifugal Milling, 2. Ball Milling, 3. Sedimentation, 4. Sieving

with 1-propanol to create a dispersion of approx. 0.1 wt% of solids. 1-propanol was used instead of ethanol or 2-propanol because of its better dispersion performance than ethanol and lower cell toxicity than 2-propanol. This dispersion was fractionated by a combination of sedimentation and filtration.

As the intended use of the test materials is in-vitro exposure tests, we did not want to add any surfactants as these can cause cell lysis and will modify the surface of the particles, making them less comparable to those MNPs found in the environment. Due to the lack of surfactants we observed poor dispersion stability and particle agglomeration during sedimentation. This leads to sedimentation at the rate of the agglomerate and not the individual particles. This non-ideal sedimentation behaviour resulted in a top liquid layer with the smallest particle fraction (< 1 μm) and a sedimented layer with all other particle fractions. Sedimentation was repeated twice and the top layer was recovered as the smallest size fraction < 1 μm. The sedimented layer was then sequentially filtered over stainless steel sieves to retrieve the other size fractions (1–5, 5–10, 10–30, 90–180, 180–300 μm). Finally, all fractions were concentrated through ultracentrifugation to produce batches with a concentration of 20 mg/ml.

**Characterisation of the MNP test materials**

**Particle size**

The particle size distribution of all MNP fractions produced was determined by static light scattering (SLS) using a fixed refractive index for each polymer. The results of SLS are volume-based particle size distributions, from which many parameters can be derived that describe the whole distribution of the size, as illustrated in Fig. 2.

Several possible definitions can be used to determine the mean size of particles in a batch of MNPs. Each definition is related to a different functionality. For instance, if the research interest lies in effects generated by the mass of the MNPs, then the volume average should be taken, whereas if the research interests are focussed more on number or surface area, a different definition of the particle size should be used. The number and volume distributions are so different due to the fact the volume is to the power 3. This means that the volume distribution is heavily biased towards larger particles, i.e. one 10 μm particle give the same volume intensity as one thousand 1 μm particles. This means that small particles can easily get outweighed in the distribution by a couple of large particles. For the number distribution, one 10 μm particle gives the same intensity as one 1 μm particle. Both distributions are important depending on what information is required by the user, therefore both have been presented. The following particle parameters have been measured and calculated for the produced MNP batches [35]:

- $D_N = \left[ \frac{\sum D_n x_n}{\sum x_n} \right]$  Number mean diameter
- $D[4, 3] = \frac{\sum D_n^4 x_n}{\sum D_n^3 x_n}$  Volume mean diameter
- $D[3, 2] = \frac{\sum D_n^3 x_n}{\sum D_n^2 x_n}$  Surface area mean diameter
- $D[2, 1] = \frac{\sum D_n^2 x_n}{\sum D_n x_n}$  Length mean diameter
- $D[1, 0] = \frac{\sum D_n x_n}{\sum x_n}$  Number mean diameter (=  $D_N$ )
- $D_{50} = D_{median}$
- $N_W$  number of particles per gram plastics (#/g)
- $A_W$  surface area of particles per gram plastics (cm<sup>2</sup>/g)
- $V_W$  volume of particles per gram plastics (cm<sup>3</sup>/g)
- $f_N(< 1)$  fraction number of particles below 1 μm
- $f_N(1 - 5)$  fraction number of particles between 1–5 μm
- $f_N(5 - 10)$  fraction number of particles between 5–10 μm
- $f_N(> 10)$  fraction number of particles larger than 10 μm

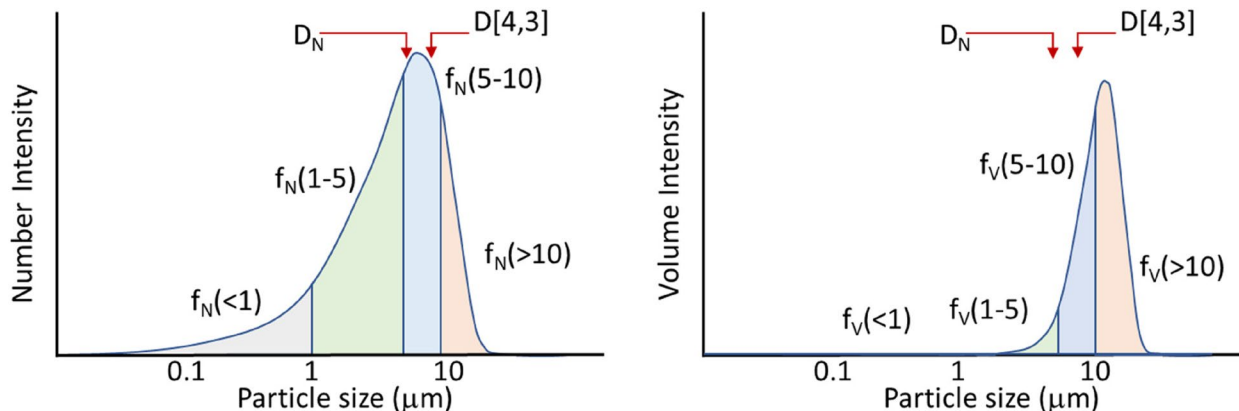


**Fig. 2** Simulated Weibull distributions for number and volume intensity, with average particle sizes  $D_N$  (number mean diameter) and  $D[4,3]$  (volume mean diameter), and fractions of particles ( $f_x$ ) within a certain size range

**Table 2** Average particle sizes calculated from the SLS experiments for PVC, including standard deviation. A standard deviation of 0.00 means < 0.005. All sizes given in  $\mu\text{m}$

	D[4,3]	D[3,2]	D[2,1]	D[1,0]=DN	D50 <sub>N</sub>	D50 <sub>V</sub>
PVC < 1	8.87 ± 0.25	2.82 ± 0.36	0.59 ± 0.05	0.28 ± 0.01	0.21 ± 0.00	5.72 ± 0.86
PVC 1–5	6.34 ± 0.10	3.99 ± 0.01	2.66 ± 0.05	1.82 ± 0.05	1.47 ± 0.08	4.65 ± 0.03
PVC 5–10	16.89 ± 1.18	9.26 ± 0.70	6.17 ± 0.14	4.92 ± 0.06	4.17 ± 0.11	10.61 ± 2.45
PVC 10–30	104.30 ± 9.22	44.89 ± 3.08	22.96 ± 0.36	17.58 ± 0.01	14.9 ± 0.02	106.48 ± 13.10
PVC 90–180	149.19 ± 0.31	138.11 ± 0.35	129.07 ± 0.33	121.34 ± 0.29	110.54 ± 0.02	133.31 ± 0.25
PVC 180–300	195.86 ± 0.53	187.47 ± 0.49	180.10 ± 0.49	172.90 ± 0.52	159.56 ± 0.66	182.41 ± 0.09

**Table 3** Fractions of PVC particles within the specified ranges for both number and volume distribution. A standard deviation of 0.0 means < 0.05. All sizes given in  $\mu\text{m}$ , fractions given as percentages (%)

	f <sub>N</sub> (< 1)	f <sub>N</sub> (1–5)	f <sub>N</sub> (5–10)	f <sub>N</sub> (> 10)	f <sub>V</sub> (< 1)	f <sub>V</sub> (1–5)	f <sub>V</sub> (5–10)	f <sub>V</sub> (> 10)
PVC < 1	98.1 ± 0.4	1.9 ± 0.3	0.1 ± 0.0	0	5.8 ± 1.1	40.5 ± 3.7	20.5 ± 1.6	33.2 ± 6.5
PVC 1–5	30.5 ± 1.5	67.4 ± 1.4	2.0 ± 0.1	0.1 ± 0.0	0.8 ± 0.1	53.4 ± 0.6	32.2 ± 0.1	13.5 ± 0.3
PVC 5–10	0	67.9 ± 2.1	30.0 ± 2.5	2.1 ± 0.4	0	15.4 ± 1.6	35.3 ± 5.5	49.4 ± 7.1
PVC 10–30	0	0	9.5 ± 0.3	90.5 ± 0.3	0	0	0.5 ± 0.1	99.5 ± 0.1
PVC 90–180	0	0	0	100	0	0	0	100
PVC 180–300	0	0	0	100	0	0	0	100

**Table 4** Average particle sizes calculated from the SLS experiments for PP/Talc, including standard deviation. A standard deviation of 0.00 means < 0.005. All sizes given in  $\mu\text{m}$

	D[4,3]	D[3,2]	D[2,1]	D[1,0]=DN	D50 <sub>N</sub>	D50 <sub>V</sub>
PP/Talc < 1	8.10 ± 0.16	3.27 ± 0.26	1.18 ± 0.21	0.59 ± 0.11	0.40 ± 0.08	5.83 ± 0.16
PP/Talc 1–5	8.35 ± 0.10	6.58 ± 0.00	5.57 ± 0.01	4.96 ± 0.01	4.28 ± 0.00	6.36 ± 0.01
PP/Talc 5–10	27.36 ± 0.96	21.88 ± 0.23	16.90 ± 0.28	12.88 ± 0.58	10.57 ± 0.58	24.16 ± 0.46
PP/Talc 90–180	142.39 ± 5.85	116.48 ± 5.67	75.90 ± 12.80	24.31 ± 9.51	6.25 ± 0.65	127.15 ± 4.77
PP/Talc 180–300	420.13 ± 0.80	323.27 ± 0.37	254.62 ± 0.10	211.18 ± 0.38	181.18 ± 0.36	326.84 ± 0.79

**Table 5** Fractions of PP/Talc particles within the specified ranges for both number and volume distribution. All sizes given in  $\mu\text{m}$ , fractions given as percentages (%)

	f <sub>N</sub> (< 1)	f <sub>N</sub> (1–5)	f <sub>N</sub> (5–10)	f <sub>N</sub> (> 10)	f <sub>V</sub> (< 1)	f <sub>V</sub> (1–5)	f <sub>V</sub> (5–10)	f <sub>V</sub> (> 10)
PP/Talc < 1	88.5 ± 4.8	11.3 ± 4.7	0.2 ± 0.1	0	5.8 ± 1.0	38.4 ± 0.1	27.6 ± 0.3	28.2 ± 1.3
PP/Talc 1–5	0	68.4 ± 0.2	30.2 ± 0.2	1.3 ± 0.1	0	27.2 ± 0.2	50.6 ± 0.2	21.7 ± 0.1
PP/Talc 5–10	0	9.1 ± 3.1	36.5 ± 1.4	54.4 ± 4.5	0	0.2 ± 0.1	4.5 ± 0.1	95.3 ± 0.2
PP/Talc 90–180	0	26.8 ± 9.4	46.1 ± 2.8	27.1 ± 12.2	0	0	0.1 ± 0.1	99.9 ± 0.1
PP/Talc 180–300	0	0	0	100	0	0	0	100

than 10  $\mu\text{m}$  f<sub>V</sub>(< 1) fraction volume of particles below 1  $\mu\text{m}$  f<sub>V</sub>(1–5) fraction volume of particles between 1–5  $\mu\text{m}$  f<sub>V</sub>(5–10) fraction volume of particles between 5–10  $\mu\text{m}$  f<sub>V</sub>(> 10) fraction volume of particles larger than 10  $\mu\text{m}$

Tables 2, 3, 4, 5 and 6 show the average particle sizes, fractions, and number, surface area and volume per gram of all the MNP batches. It can be seen that for most batches the number mean diameters (D[1,0]) correspond well to the desired size of the batches, demonstrating

**Table 6** Number, surface area and volume per gram of dry particles

	$N_w$ (#/g)	$A_w$ (cm <sup>2</sup> /g)	$V_w$ (cm <sup>3</sup> /g)		$N_w$ (#/g)	$A_w$ (cm <sup>2</sup> /g)	$V_w$ (cm <sup>3</sup> /g)
PVC <1	$3.2 \pm 0.8 \cdot 10^{12}$	$15,200 \pm 1520$	0.72	PP/Talc <1	$8.0 \pm 4.0 \cdot 10^{11}$	$16,400 \pm 920$	0.89
PVC 1–5	$6.8 \pm 0.7 \cdot 10^{10}$	$10,900 \pm 22$	0.72	PP/Talc 1–5	$9.3 \pm 0.1 \cdot 10^9$	$8080 \pm 100$	0.89
PVC 5–10	$4.9 \pm 0.5 \cdot 10^9$	$4720 \pm 360$	0.72	PP/Talc 5–10	$3.5 \pm 0.3 \cdot 10^8$	$2430 \pm 26$	0.89
PVC 10–30	$7.7 \pm 0.6 \cdot 10^7$	$973 \pm 67$	0.72				
PVC 90–180	$6.4 \pm 0.0 \cdot 10^5$	$315 \pm 0.8$	0.72	PP/Talc 90–180	$9.9 \pm 6.5 \cdot 10^6$	$458 \pm 22$	0.89
PVC 180–300	$2.4 \pm 0.0 \cdot 10^5$	$232 \pm 0.6$	0.72	PP/Talc 180–300	$9.7 \pm 0.1 \cdot 10^4$	$165 \pm 0$	0.89

that the milling and fractionation procedure produces suitable test materials. There are four cases where this is not the case: the D[1,0] for PVC 5–10, PVC 90–180 and PP 90–180 is slightly smaller and for PP 5–10 is slightly larger than expected. This is also reflected in the number fractions where it can be seen that the majority of the particles are in the desired fraction, with PVC batches generally having more particles in the desired fraction than the respective PP/Talc sample. Finally, the surface area is calculated based on a smooth, spherical, non-porous particle. Whilst this is not a completely accurate representation of the true particles, it is hoped that such information will aid in estimating surface area dependent effects such as biofilm formation and MNPs as pathogenic or chemical vectors.

**Quantification of filler materials**

Thermogravimetric Analysis (TGA) was used to investigate the presence of inorganic fillers in the test materials. This is especially important for the PP. For both plastics, the <1 and 90–180 μm batches were tested and TGA traces are shown in Fig. 3. The PVC shows two mass loss events. The first, between 200 and 400 °C indicates the loss of HCl and the second, between 400 and 600 °C is the pyrolysis of the carbon chain. The residual mass is

most likely carbon fragments that are formed during the HCl release and cannot be further pyrolyzed. The difference between the smaller and larger particles is due to the particle size. The smaller particles generally pyrolyze faster and more completely due to their larger surface to volume ratio.

The PP/Talc shows a single weight loss event around 450 °C corresponding to pyrolysis of the polymer. There is a clear difference in residual weight between the larger and the smaller particles. The larger particles have a much lower residual weight than the smaller particles. The residual weights are shown in Table S1. The fraction of talc blended in the polypropylene during production was 30 wt%, whereas after milling the talc content is shown to be 26.2% for the larger particles and 41.6% for the smaller particles. As the size of the talc particles is 100–300 nm, this suggests that a fraction of the PP/Talc <1 μm batch may be talc particles that have been released from the PP during grinding, and are no longer embedded in a PP matrix.

**Chemical composition and contamination**

The chemical composition of two batches of PVC and two batches of PP/Talc was investigated after milling (see Table 1 for milling conditions of the corresponding

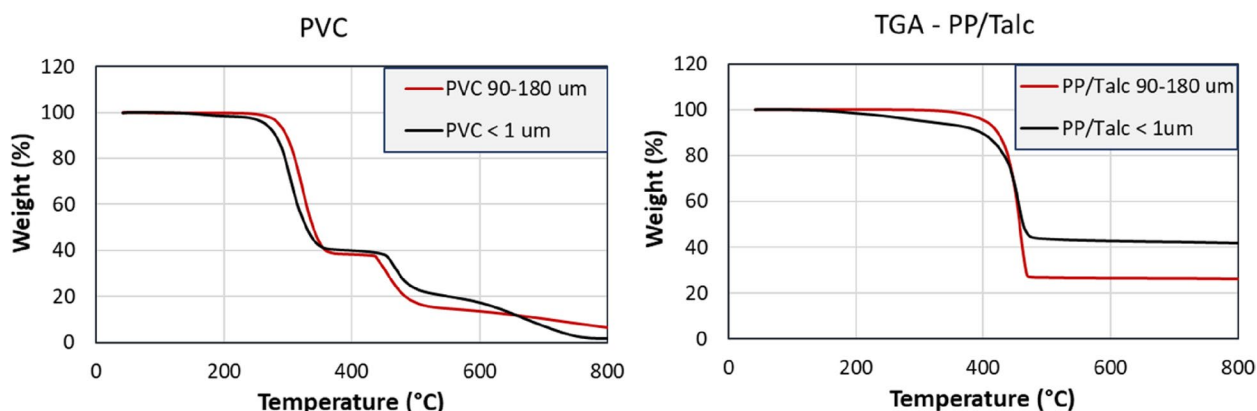


**Fig. 3** TGA traces of large and small PVC and PP/Talc fractions

batches) using X-ray Fluorescence (XRF). These results are shown in Table S2. In all batches the total contaminant concentration is <1 wt%. Ca and Zn are present in both polymers as stabilizers, as is the P in PVC. Fe, Cr and Ni are components of stainless steel which are possibly released either from the centrifugal mill or a small stainless steel mesh in the ball-milling vessel. The Zr and Y are likely introduced by the ball-milling components (beads, stirrer and vessel) which are made of Y-stabilized ZrO<sub>2</sub>. The higher load of Zr in the PVC\_BIII batch may be due to use of new beads for that batch. The higher concentration of Fe in the PP/Talc may be due to the higher abrasivity of the talc against the stainless steel mesh in the grinding vessel. The presence of other unexplained contaminants is low, totalling <0.5 wt% in PVC (mainly due to the high Na content) and <0.01 wt% for PP/Talc.

#### Single particle physicochemical analysis

SEM–EDX analyses were performed in order to characterise the morphology of the particles and to investigate contaminations on the single particle level. Figure 4 shows representative particles from the batches <1, 1–5 and 5–10 μm of PVC and PP/Talc. Further images are available in Figures S1, S2, S3, S4, S5 and S6 of the Supplementary Information. Multiple morphologies are observed, both due to size and plastic type. Particles

of both PP/Talc and PVC in the fraction <1 μm appear to have a smoother, rounder morphology than particles >1 μm. In the fractions 1–5 and 5–10 μm there are differences observed between the two plastics. PP/Talc particles appear to be flatter and irregular in shape with sharper edges in the fraction 1–5 μm and fibre-like structures protruding from the edges in particles >10 μm. In contrast, PVC particles are also irregular in shape but more rounded edges than PP in the fraction 1–5 μm, whilst the fraction 5–10 μm appears to be larger aggregates of small, round particles. Further characterisation of the 3D structure of the particles, specifically to quantify the thickness of particles, would be very useful but has thus far been unsuccessful with SEM and a tilted stage. Further research could focus on using AFM to quantify width vs height, or with confocal fluorescence microscopy if the particles were labelled.

Using back-scattered electron (BSE) detectors, contrast arises due to the atomic number of the element(s) under observation, known as Z-contrast [36]. This may be used to identify local metal contaminants on a single particle level. Figures S7a + b in the supporting information show secondary electron (SE) and BSE images of a PVC particle from the 1–5 μm batch. In the SE image the same globular aggregate morphology is observed as described above for the fraction 5–10 μm, however, in the BSE

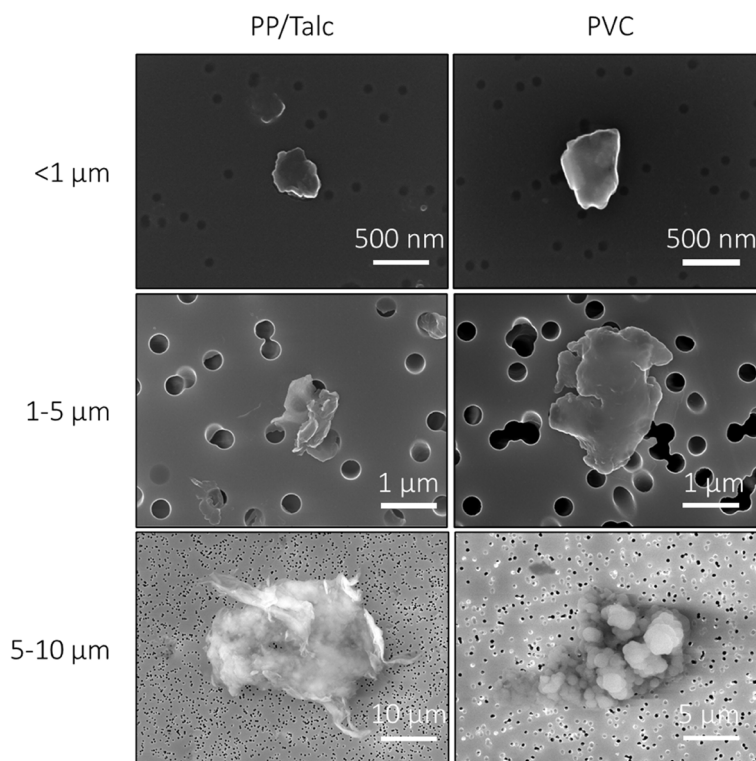


**Fig. 4** Secondary electron SEM images of PP/Talc and PVC particles in the size fractions <1, 1–5 and 5–10 μm

image small bright spots are visible which may be indicative of metal contamination. EDX of one of these spots, shown in Figure S7c shows that these spots contain Zr. This, in combination with the XRF results, shows that Zr contamination is present in low levels on some of the PVC particles. It should be noted that this is observed on fewer than half of the particles.

**Stability of MNP suspensions**

Two types of stability can be assessed, the long-term (shelf life) stability of the MNP in 1-propanol during storage in a refrigerator (4 °C) and the stability of the MNP when diluted in the presence of BSA (in-use). The final samples of (20 mg/ml) MNPs in 1-propanol were made on day 0, and tested on days 0 and 46. After 58 days the particles were transferred to BSA and measured immediately and after 13, 48 and 218 days. The particle size distributions can be seen in Fig. 5.

Both MNP materials show some changes in particle size distribution in time. The PVC 1–5 μm indicates some agglomeration in 1-propanol over time, but after dispersing in BSA some of the small agglomerates

break up and form a larger number of small particles. The fraction <1 μm is 30% in the fresh sample whilst this is increased to 52% after 276 days. The same size development of agglomeration in 1-propanol and deagglomeration in BSA can be seen in the PP/Talc <1 μm sample. Blank SLS measurements of the 0.05 wt% BSA solution without MNPs were performed, however the concentration of possible proteins and protein agglomerates was too low to measure, therefore the particle size information presented is representative of the MNPs themselves.

The development of the number average particle size of both materials are shown in Fig. 6. The number average size of PVC decreases slightly with time for the PVC 1–5 μm sample, however the PVC <1 μm increases in size. The number average particle size of the PP/Talc 1–5 μm shows a bigger change with a large decrease in size over the first two months. This is possibly due to some of the talc particles being released from the material, which may result in a significant lowering of the average particle size. For both plastics, after dispersion in BSA the particle size remains constant for 31 weeks.

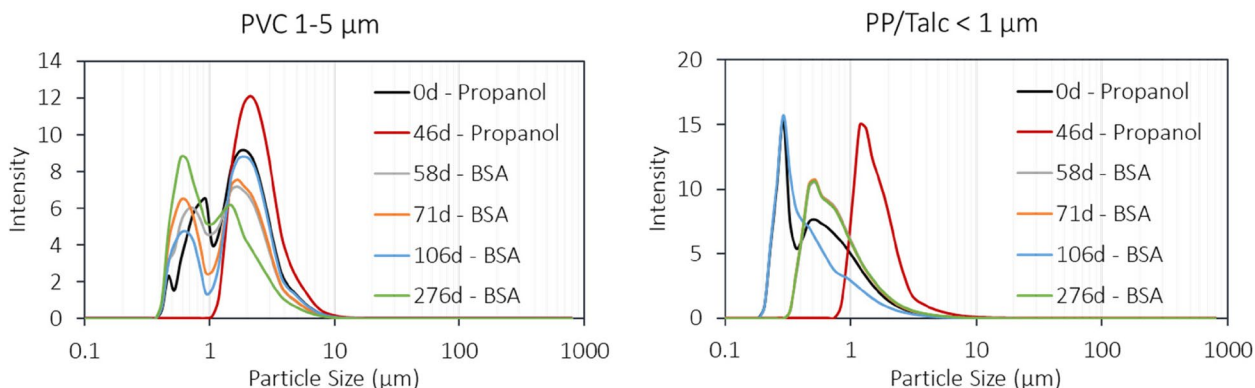


**Fig. 5** Change in number distribution of PVC 1–5 μm and PP/Talc <1 μm during storage and cell medium stability testing

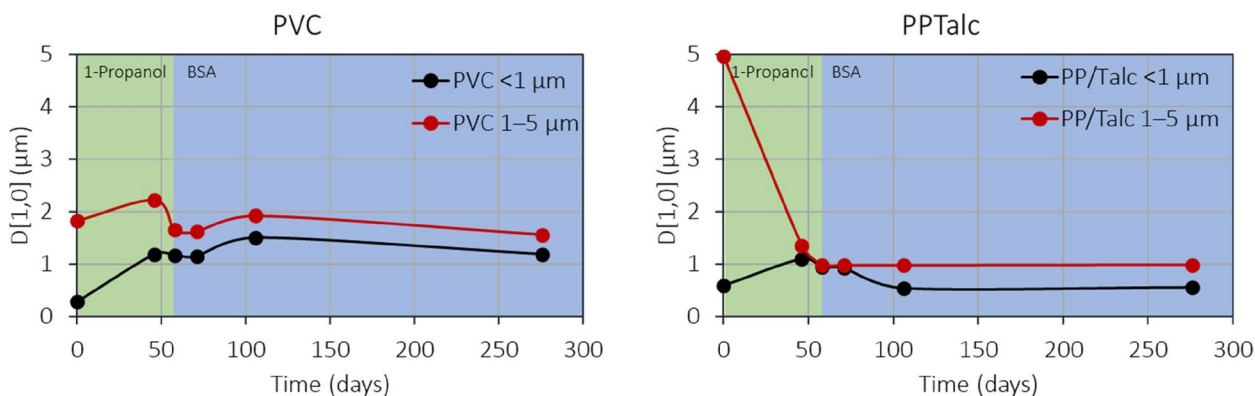


**Fig. 6** Number average particle size development of PVC and PP/Talc with time in 1-propanol and BSA



## Conclusions

We have successfully demonstrated a protocol to prepare suitable micro- and nanoplastic test materials. Through a two-step milling process followed by sedimentation and sieving, fractions with narrow size distributions of particles between <1, 1–5, 5–10, 10–30, 90–180 and 180–300  $\mu\text{m}$  were created. These particles were shown to have low levels of contaminants containing elements originating from stainless steel and  $\text{ZrO}_2$  apparatus that was used during preparation. The produced particles were also tested for stability in both 1-propanol (storage) and 0.05 wt% BSA solution (test matrix) for up to 9 months. After initial agglomeration in 1-propanol, the particles are stable in BSA although some changes in time can be seen due to the breakup of agglomerates. Whilst this work has focused on producing PVC and PP/Talc test materials, we hope that it may be easily applied to other plastics when test materials are needed. It is important to note that when using such test materials suitable controls should also be prepared. For example, the talc additive on its own and 1-propanol that has been used for milling and sedimentation to account for the leaching of additives during the process.

## Materials and methods

### Materials

PVC (SigmaAldrich Merck, no. 346764, Mw-233000, powder), Polypropylene with 30 wt% talc (LyondellBasell, pellet), ethanol (Thermo Scientific, Technical grade 96%), 1-propanol (SigmaAldrich Merck, nr. 402,893, 99.5%), MilliQ water, BSA (SigmaAldrich nr. A7906) and Phosphate-buffer saline (PBS) (Gibco nr. 18,912–014, 1 tablet per 500 ml demiwater) were all used as received without further purification with the exception of the MilliQ water which was filtered using a Millipore 0.22  $\mu\text{m}$  filter. The talc filler for the polypropylene was supplied by Nanoshel (Talc nanoparticles, <100 nm, 99.9% purity).

### Milling

The centrifugal milling was performed using a Retsch ZM100 centrifugal mill with a 500  $\mu\text{m}$  screen. Milling was performed either at room temperature or under  $\text{LN}_2$ . Ball-milling was performed using a Dispermat ball mill (VMA-Getzmann GmbH) using Y-stabilised  $\text{ZrO}_2$  beads (E&R BV), a  $\text{ZrO}_2$  vessel and  $\text{ZrO}_2$  double impeller rotor. Ball-milling was performed for between 1–25 h, at between 2000–6000 rpm either a room temperature or under  $\text{LN}_2$  and in ethanol or 1-propanol. Full details are described in the main text.

### Fractionation

Sedimentation was performed twice in 1-propanol using a 30 cm glass column with a diameter of 8 cm.

Larger particles were allowed to sediment for ~16 h before removing smaller particles from the supernatant. Sieving was performed wet using stainless steel sieves of 5 and 20, 30, 90, 180 and 300  $\mu\text{m}$  with diameter 4–5 cm.

### Preparation of suspensions in 0.05 wt% BSA solution

The MNPs were manually shaken and 10  $\mu\text{l}$  (20 mg/ml) was added to 300  $\mu\text{l}$  BSA solution (0.5 wt%). This was manually shaken for 1 min and then diluted with 2700  $\mu\text{l}$  MilliQ water resulting in 3 ml MNP in 0.05 wt% BSA solution (~60  $\mu\text{g}/\text{ml}$ ).

### Determination of particle stability

For the assessment of shelf life stability in 1-propanol, the stock dispersions of 20 mg/ml were regularly retrieved from the refrigerator and manually shaken to redisperse the particles. For the stability in the presence of BSA, a working suspension of ~60  $\mu\text{g}/\text{ml}$  MNP in 0.05 wt% BSA solution was prepared and stored in a refrigerator (4°C). The particle size distribution of this working suspension was measured without further modification.

### Static Light Scattering (SLS)

SLS was performed using a Shimadzu SALD 7500nano with a 405 nm laser, that has the possibility of measuring particle size between 7 nm and 800  $\mu\text{m}$ . The dispersions were diluted in 1-propanol and measured under constant movement at laboratory conditions (23 °C, ~50% relative humidity). The refractive indices used for the calculation of the particle size distributions from the scattering results were 1.55–0.001 for PVC and 1.60–0.001 for PP/Talc, respectively.

### Scanning electron microscopy with energy dispersive x-ray spectroscopy

SEM–EDX analyses were performed with a Tescan MAIA III Triglav field emission scanning electron microscope, equipped with Bruker XFlash Quantax 30  $\text{mm}^2$  silicon drift detectors for energy dispersive X-ray spectroscopy. SEM images were recorded in the secondary electron (SE) and backscattered electron (BSE) modes between 5–15 kV.

### Thermogravimetric Analysis (TGA)

TGA was used to determine the fraction of inorganic additives in the polymers. The equipment used was the TA Instruments TGA5500. The experiments were performed under nitrogen with a heating rate of 20 °C/min from room temperature up to 800 °C. The mass loss with time and temperature is monitored. Two of the

PP/Talc and two of the PVC batches were assessed for their weight loss.

### X-ray Fluorescence (XRF)

The composition and contamination of the MNPs were assessed by means of XRF spectroscopy, using a MalvernPanalytical Epsilon 4 benchtop analyser and Omnian software. The benefit of this chemical characterization technique is the measurement of the average composition over a relatively large sample. This is also the major drawback, because large volumes of material are needed to test. For many ground samples, the mass produced (especially the batches of smaller particles) was low, meaning that the required amount was not available.

### Abbreviations

BSA	Bovine Serum Albumin
BSE	Back Scattered Electron
EDX	Energy Dispersive X-ray Spectroscopy
LN <sub>2</sub>	Liquid Nitrogen
MNP	Micro- and Nanoplastics
PBS	Phosphate-buffer Saline
PE	Polyethylene
PP	Polypropylene
PS	Polystyrene
PVC	Polyvinyl Chloride
SE	Secondary Electron
SEM	Scanning Electron Microscopy
SLS	Static Light Scattering
TGA	Thermogravimetric Analysis
XRF	X-ray Fluorescence
ZrO <sub>2</sub>	Zirconium Oxide

### Supplementary Information

The online version contains supplementary material available at <https://doi.org/10.1186/s43591-023-00058-2>.

**Additional file 1. Figure S1.** Additional images of PP/Talc <1 µm particles. **Figure S2.** Additional images of PP/Talc 1–5 µm particles. **Figure S3.** Additional images of PP/Talc 5–10 µm particles. **Figure S4.** Additional images of PVC <1 µm particles. **Figure S5.** Additional images of PVC 1–5 µm particles. **Figure S6.** Additional images of PVC 5–10 µm particles. **Figure S7.** Secondary electron (SE) (a) and back-scattered electron (BSE) (b) images of PVC 1–5 µm particle with Zr contamination present as white spots in the BSE image. EDX of the particles (c) shows the Zr Kα peak at 15.744 keV. The larger Zr Lα peak at 2.042 keV is obscured by the Au M peak at 2.120 keV present due to the filter material. **Table S1.** Residual mass at 800 °C derived from the TGA experiments. **Table S2.** Composition and contamination of four ground polymer batches as determined by XRF.

### Acknowledgements

The authors would like to thank Erik Rushton and Mara Destro (LyondellBasell) for the PP/Talc starting material Taco van der Maten (Malvern Panalytical) for the XRF analysis, Marloes van Os (TNO) for additional SEM measurements, Petra Krystek (Deltareis) for helping set-up the project and Jens Reiber (Wessling) for fruitful discussion.

### Authors' contributions

Conceptualization, S.H., I.M.K. and A.B.; methodology, A.B.; investigation, L.A.P., E.M.H., E.F.v.A., K.G. and M.G.A.N.; writing—original draft preparation, L.A.P. and A.B.; writing—review and editing, E.M.H., S.H., M.G.A.N. and A.M.B.; visualization, L.A.P., E.M.H., E.F.v.A. and A.B.; supervision, L.A.P., A.M.B. and A.B.; project

administration, S.H. and A.M.B.; funding acquisition, S.H., I.M.K. and A.B. All authors read and approved the final manuscript.

### Funding

This research was funded by ZonMw and Health Holland through the Microplastics and Human Health consortium MOMENTUM (grant ID: 458001101).

### Availability of data and materials

The datasets used and/or analysed during the current study are available from the corresponding author on reasonable request.

### Declarations

#### Ethics approval and consent to participate

Not applicable.

#### Consent for publication

All authors consent to publication.

#### Competing interests

The authors declare no conflict of interest.

Received: 22 December 2022 Accepted: 27 April 2023

Published online: 05 May 2023

### References

- Hartmann NB, Hüffer T, Thompson RC, Hasselöv M, Verschoor A, Daugaard AE, Rist S, Karlsson T, Brennholt N, Cole M, Herrling MP, Hess MC, Ivleva NP, Lusher AL, Wagner M. Are We Speaking the Same Language? Recommendations for a Definition and Categorization Framework for Plastic Debris. *Environ Sci Technol*. 2019;53:1039–47. [https://doi.org/10.1021/ACS.EST.8B05297/ASSET/IMAGES/MEDIUM/ES-2018-05297K\\_0006.GIF](https://doi.org/10.1021/ACS.EST.8B05297/ASSET/IMAGES/MEDIUM/ES-2018-05297K_0006.GIF).
- Ekvall MT, Lundqvist M, Kelpsiene E, Šileikis E, Gunnarsson SB, Cedervall T. Nanoplastics formed during the mechanical breakdown of daily-use polystyrene products. *Nanoscale Adv*. 2019;1:1055–61. <https://doi.org/10.1039/C8NA00210J>.
- Ward CP, Reddy CM. We need better data about the environmental persistence of plastic goods. *Proc Natl Acad Sci U S A*. 2020;117:14618–21. <https://doi.org/10.1073/PNAS.2008009117/-/DCSUPPLEMENTAL>.
- Chamas A, Moon H, Zheng J, Qiu Y, Tabassum T, Jang JH, Abu-Omar M, Scott SL, Suh S. Degradation Rates of Plastics in the Environment. *ACS Sustain Chem Eng*. 2020;8:3494–511. <https://doi.org/10.1021/acssuschemeng.9b06635>.
- Koelmans AA, Nor NHM, Hermsen E, Kooi M, Mintenig SM, De France J. Microplastics in freshwaters and drinking water: Critical review and assessment of data quality. *Water Res*. 2019;155:410–22. <https://doi.org/10.1016/j.watres.2019.02.054>.
- Ugwu K, Herrera A, Gómez M. Microplastics in marine biota: A review. *Mar Pollut Bull*. 2021;169:112540. <https://doi.org/10.1016/j.marpolbul.2021.112540>.
- Munyaneza J, Jia Q, Qaraah FA, Hossain MF, Wu C, Zhen H, Xiu G. A review of atmospheric microplastics pollution: In-depth sighting of sources, analytical methods, physiognomies, transport and risks. *Sci Total Environ*. 2022;822:153339. <https://doi.org/10.1016/j.scitotenv.2022.153339>.
- Gasperi J, Wright SL, Dris R, Collard F, Mandin C, Guerrouache M, Langlois V, Kelly FJ, Tassin B. Microplastics in air: Are we breathing it in? *Curr Opin Environ Sci Heal*. 2018;1:1–5. <https://doi.org/10.1016/j.coesh.2017.10.002>.
- O'Connor JD, Mahon AM, Ramsperger AFRM, Trotter B, Redondo Hasselerharm PE, Koelmans AA, Lally HT, Murphy SA. Microplastics in Freshwater Biota: A Critical Review of Isolation, Characterization, and Assessment Methods. *Glob Chall*. 2020;4:1800118. <https://doi.org/10.1002/GCH2.201800118>.
- Azeem I, Adeel M, Ahmad MA, Shakoor N, Jiangcuo GD, Azeem K, Ishfaq M, Shakoor A, Ayaz M, Xu M, Rui Y. Uptake and Accumulation of Nano/Microplastics in Plants: A Critical Review. *Nanomater*. 2021;11:2935. <https://doi.org/10.3390/NANO11112935>.

11. Leslie HA, van Velzen MJM, Brandsma SH, Vethaak AD, Garcia Vallejo JJ, Lamoree MH. Discovery and quantification of plastic particle pollution in human blood. *Environ Int.* 2022;163:107199. <https://doi.org/10.1016/j.envint.2022.107199>.
12. Ragusa A, Svelato A, Santacroce C, Catalano P, Notarstefano V, Carnevali O, Papa F, Rongioletti MCA, Baiocco F, Draghi S, D'Amore E, Rinaldo D, Matta M, Giorgini E. Plasticenta: First evidence of microplastics in human placenta. *Environ Int.* 2021;146:106274. <https://doi.org/10.1016/j.envint.2020.106274>.
13. Vethaak AD, Legler J. Microplastics and human health. *Science.* 2021;371:672–4. <https://doi.org/10.1126/science.abe5041>.
14. Leslie HA, Depledge MH. Where is the evidence that human exposure to microplastics is safe? *Environ Int.* 2020;142:105807. <https://doi.org/10.1016/j.envint.2020.105807>.
15. Donkers JM, Höppener EM, Grigoriev I, Will L, Melgert BN, van der Zaan B, van de Steeg E, Kooter IM. Advanced epithelial lung and gut barrier models demonstrate passage of microplastic particles. *Microplastics Nanoplastics.* 2022;2:1–18. <https://doi.org/10.1186/S43591-021-00024-W>.
16. Beijer NRM, Dehaut A, Carlier MP, Wolter H, Versteegen RM, Pennings JLA, de la Fonteyne L, Niemann H, Janssen HM, Timmermans BG, Mennes W, Cassee FR, Mengelers MJB, Amaral-Zettler LA, Duflos G, Staal YCM. Relationship Between Particle Properties and Immunotoxicological Effects of Environmentally-Sourced Microplastics. *Front Water.* 2022;4:66. <https://doi.org/10.3389/frwa.2022.866732/BIBTEX>.
17. Dusza HM, Katrukha EA, Nijmeijer SM, Akhmanova A, Vethaak AD, Walker DJ, Legler J. Uptake, Transport, and Toxicity of Pristine and Weathered Micro- and Nanoplastics in Human Placenta Cells. *Environ Health Perspect.* 2022;130:97006. <https://doi.org/10.1289/EHP10873>.
18. de Ruijter VN, Redondo-Hasselerharm PE, Gouin T, Koelmans AA. Quality Criteria for Microplastic Effect Studies in the Context of Risk Assessment: A Critical Review. *Environ Sci Technol.* 2020;54:11692–705. <https://doi.org/10.1021/acs.est.0c03057>.
19. A.A. Koelmans, P.E. Redondo-Hasselerharm, N. Hazimah Mohamed Nor, V.N. Ruijter, S.M. Mintenig, M. Kooi. Risk assessment of microplastic particles. (n.d.). <https://doi.org/10.1038/s41578-021-00411-y>.
20. A. Boobis, F. Cassee, T. Gouin, A.A. Koelmans, S. Price, S. Wagener, S.L. Wright. Dietary and inhalation exposure to nano- and microplastic particles and potential implications for human health. 2022. <https://www.who.int/publications/i/item/9789240054608> (Accessed 21 Dec 2022).
21. Burns EE, Boxall ABA. Microplastics in the aquatic environment: Evidence for or against adverse impacts and major knowledge gaps. *Environ Toxicol Chem.* 2018;37:2776–96. <https://doi.org/10.1002/ETC.4268>.
22. Kooi M, Koelmans AA. Simplifying Microplastic via Continuous Probability Distributions for Size, Shape, and Density. *Environ Sci Technol Lett.* 2019;6:551–7. <https://doi.org/10.1021/acs.estlett.9b00379>.
23. Arechabala B, Coiffard C, Rivalland P, Coiffard LJM, De Roeck-Holtzhauer Y. Comparison of cytotoxicity of various surfactants tested on normal human fibroblast cultures using the neutral red test, MTT assay and LDH release. *J Appl Toxicol.* 1999;19:163–5. [https://doi.org/10.1002/\(SICI\)1099-1263\(199905/06\)19:3%3c163::AID-JAT561%3e3.0.CO;2-H](https://doi.org/10.1002/(SICI)1099-1263(199905/06)19:3%3c163::AID-JAT561%3e3.0.CO;2-H).
24. Cai H, Xu EG, Du F, Li R, Liu J, Shi H. Analysis of environmental nanoplastics: Progress and challenges. *Chem Eng J.* 2021;410:128208. <https://doi.org/10.1016/j.cej.2020.128208>.
25. Ogonowski M, Schür C, Jarsén Á, Gorokhova E. The effects of natural and anthropogenic microparticles on individual fitness in *Daphnia magna*. *PLoS One.* 2016;11:155063. <https://doi.org/10.1371/journal.pone.0155063>.
26. Tanaka K, Takahashi Y, Kuramochi H, Osako M, Tanaka S, Suzuki G. Preparation of nanoscale particles of five major polymers as potential standards for the study of nanoplastics. *Small.* 2021;17:e2105781. <https://doi.org/10.1002/SMLL.202105781>.
27. Rodríguez-Hernández AG, Muñoz-Tabares JA, Aguilar-Guzmán JC, Vazquez-Duhalt R. A novel and simple method for polyethylene terephthalate (PET) nanoparticle production. *Environ Sci Nano.* 2019;6:2031–6. <https://doi.org/10.1039/c9en00365g>.
28. Balakrishnan G, Déniel M, Nicolai T, Chassenieux C, Lagarde F. Towards more realistic reference microplastics and nanoplastics: preparation of polyethylene micro/nanoparticles with a biosurfactant. *Environ Sci Nano.* 2019;6:315–24. <https://doi.org/10.1039/C8EN01005F>.
29. Mitrano DM, Beltzung A, Frehland S, Schmiedgruber M, Cingolani A, Schmidt F. Synthesis of metal-doped nanoplastics and their utility to investigate fate and behaviour in complex environmental systems. *Nat Nanotechnol.* 2019;14:362–8. <https://doi.org/10.1038/s41565-018-0360-3>.
30. El Hadri H, Gigault J, Maxit B, Grassl B, Reynaud S. Nanoplastic from mechanically degraded primary and secondary microplastics for environmental assessments. *Nanoplastics.* 2020;17:100206. <https://doi.org/10.1016/j.nanoplast.2019.100206>.
31. Caldwell J, Lehner R, Balog S, Rheme C, Gao X, Septiadi D, Weder C, Petri-Fink A, Rothen-Rutishauser B. Fluorescent plastic nanoparticles to track their interaction and fate in physiological environments. *Environ Sci Nano.* 2021;8:502–13. <https://doi.org/10.1039/d0en00944j>.
32. Seghers J, Stefaniak EA, La Spina R, Cella C, Mehn D, Gilliland D, Held A, Jacobsson U, Emteborg H. Preparation of a reference material for microplastics in water—evaluation of homogeneity. *Anal Bioanal Chem.* 2022;414:385–97. <https://doi.org/10.1007/S00216-021-03198-7/FIGURES/6>.
33. Lapcik L, Jindrova P, Lapcikova B, Tamblyn R, Greenwood R, Rowson N. Effect of the talc filler content on the mechanical properties of polypropylene composites. *J Appl Polym Sci.* 2008;110:2742–7. <https://doi.org/10.1002/APP.28797>.
34. Maiti SN, Sharma KK. Studies on polypropylene composites filled with talc particles - Part I Mechanical properties. *J Mater Sci.* 1992;27:4605–13. <https://doi.org/10.1007/BF01165994/METRICS>.
35. ISO, 9276–2:2014. Representation of results of particle size analysis — Part 2: Calculation of average particle sizes/diameters and moments from particle size distributions. International Organisation for Standardisation; 2014.
36. Lloyd GE. Atomic number and crystallographic contrast images with the SEM: a review of backscattered electron techniques. *Mineral Mag.* 1987;51:3–19. <https://doi.org/10.1180/MINMAG.1987.051.359.02>.

## Publisher's Note

Springer Nature remains neutral with regard to jurisdictional claims in published maps and institutional affiliations.

Submit your manuscript to a SpringerOpen® journal and benefit from:

- Convenient online submission
- Rigorous peer review
- Open access: articles freely available online
- High visibility within the field
- Retaining the copyright to your article

Submit your next manuscript at ► [springeropen.com](https://www.springeropen.com)